Chemically exfoliated large-area two-dimensional flakes of molybdenum disulfide for device applications

Vivek Pachauri', Klaus Kern', and Kannan Balasubramanian'

Citation: APL Materials **1**, 032102 (2013); doi: 10.1063/1.4820423
View online: http://dx.doi.org/10.1063/1.4820423
View Table of Contents: http://aip.scitation.org/toc/apm/1/3
Published by the American Institute of Physics

Chemically exfoliated large-area two-dimensional flakes of molybdenum disulfide for device applications

Vivek Pachauri,[1,a] Klaus Kern,[1,2,b] and Kannan Balasubramanian[1,c]
[1]*Max Planck Institute for Solid State Research, Heisenbergstrasse 1, 70569 Stuttgart, Germany*
[2]*Institut de Physique de la Matière Condensée, Ecole Polytechnique Fédérale de Lausanne, 1015 Lausanne, Switzerland*

(Received 2 May 2013; accepted 26 July 2013; published online 4 September 2013)

A solution-based exfoliation method for obtaining large-area two-dimensional flakes of molybdenum disulfide, followed by the fabrication of electrical devices is presented in this manuscript. The exfoliation method is based on the use of an aprotic solvent, namely, acetonitrile under mild sonication steps. In order to fabricate devices, a dielectrophoresis technique is used for transferring MoS_2 flakes site-specifically on to the electrode pairs pre-written on the glass chips. The devices fabricated thus can be operated as chemical sensor in liquids while investigations under photo illumination indicate that such devices can also efficiently function as photodetectors. [http://dx.doi.org/10.1063/1.4820423]

The possibility to access and investigate atomic layers of a material is an interesting prospect driving many experiments around the globe. In addition to the novel physics arising out of such experiments, the physical and chemical properties of these layers show promise for new kinds of applications.[1,2] Graphene is an excellent candidate underlining this aspect, showing rich physics surpassing research on alternative systems – such as the 2D electron gas in GaAs – that have dominated for decades. Furthermore, its unique electronic structure renders it as a promising active material for a number of applications including field-effect devices, sensors, and optical components.[2–6] One major aspect hampering the widespread use of graphene is the absence of a bandgap. Many approaches are underway in order to overcome this hurdle such as the fabrication of graphene nanoribbons, or by using external fields.[7–10] Here layered inorganic materials such as MoS_2 are attracting significant amount of interest recently offering a suitable alternative due to their intrinsic bandgap. 2D MoS_2 exhibit a direct bandgap of 2 eV in contrast to an indirect bandgap of 1.8 eV for the bulk material.[11,12] MoS_2-based 2D devices have been shown as excellent field-effect transistors and logic gates operable at room temperatures suggesting their direct application in integrated circuits and other areas.[13–16] Similarly, optical properties of thin-layer MoS_2 have suggested their potential use in optoelectronics and photovoltaics.[17–20] Some theoretical studies even predict that the transfer characteristics for thin-layer MoS_2-based devices may be better than that of silicon.[21,22] Large-area thin layers of MoS_2 and other chalcogenides are also recently suggested as appropriate candidates for applications such as hydrogen catalysis, composite materials, and as anode material in new energy storage devices.[23–25]

With the scientific and application prospects scoring so high, methods for reproducibly accessing good quality thin layers of MoS_2 are required for the various applications discussed above.

[a]Present address: Department of Computer Science and Microsystem Technology, University of Applied Sciences, Kaiserslautern, Amerikastrasse 1, 66482 Zweibruecken, Germany. E-mail: vivek.pachauri@fh-kl.de
[b]Email: k.kern@fkf.mpg.de
[c]Email: b.kannan@fkf.mpg.de

Mechanical exfoliation of MoS_2 crystals followed by e-beam lithography (EBL) is the standard procedure used for the fabrication of 2D devices of MoS_2. New methods to access thin layers of MoS_2 by chemical vapor deposition (CVD), epitaxial growth, and laser thinning have been reported recently.[26–28] Alternative protocols are continuously sought for in order to overcome drawbacks such as serial processing by EBL. Examples of such methods include scalable fabrication of electrical devices on a variety of substrates using dielectrophoresis and site-specific chemical anchoring techniques.[29,30] In these cases the individual layers of the material are obtained in solution by exfoliation. The advantages offered by solution processing of layered materials include access to versatile 2D material by chemical modification and easy handling before the fabrication of the desired devices. Here it is also important to have the nanomaterial dispersions in an appropriate solvent, as otherwise the physical properties of the solvent may have an adverse effect on the stability of nanomaterials. Since the 1980s there have been rigorous activities focused on exfoliating MoS_2 in solution; however there has been little focus on methods to obtain large area flakes of thin layers of MoS_2 in appropriate solvents. Most popular methods to break down the van der Waals forces between MoS_2 layers involved the use of ion-/molecule-intercalation methods such as Li ion intercalation, side-functionalization, amine complexation, polymer conjugation, and ultrasonication in high surface tension solvents, etc.[24,31–37] While these methods are effective to some extent, they also have disadvantages yielding mainly small-sized flakes (maximum size around 1 μm) and very often affecting the chemical and physical characteristics of MoS_2 layers. Furthermore, methods using Li ions, Lewis bases and similar reduction-intensive compounds result in metallization, creation of superconducting lattices, and introduction of impurities in MoS_2.[38,39] Some recent studies have focused on using chemically mild methods for the exfoliation of MoS_2 and other dichalcogenide materials. However, they are not ideally suitable for routine device fabrication purposes due to use of high-density organic compounds as solvents. Moreover, they do not yield flakes of larger sizes, which in the case of 2D materials is very attractive for fabricating devices on a large scale.[40]

Here, we demonstrate for the first time an optimized solution-based exfoliation method to obtain a dispersion of particularly large-area flakes of thin layer MoS_2. Exfoliation of bulk MoS_2 (single crystal) is carried out under ambient conditions using acetonitrile as an aprotic solvent yielding thin layers of MoS_2 with average sizes of tens of microns and thicknesses as low as 10 nm. The exfoliation protocol involves ultrasonication and mild agitation, which were carefully optimized in order to provide optimal mechanical exertion on the MoS_2 crystal facilitating the zip-off of intact large-sized layers. The flakes obtained in this manner were subsequently incorporated in devices in a site-specific manner. For this purpose, glass chips with pre-patterned electrodes were deployed. The MoS_2 flakes were trapped in electrode gaps on the glass chip using AC dielectrophoresis. These devices were then deployed as ion-sensitive field-effect transistors (ISFETs) and could be operated as a pH sensor. Further, photoconductivity could be observed when the devices were investigated under photo illumination.

Figure 1(a) presents an overview of the exfoliation protocol used here to obtain individual flakes as dispersion (Figure 1(c)) in acetonitrile solution from MoS_2 crystal (Figure 1(b)). Figures 1(d) and 1(e) show optical images of the flakes drop-casted from dispersion on a glass slide. It is apparent that large flakes with sizes in the order of 10–60 μm are present in the dispersion. Such flakes could be repeatedly obtained with thickness ranging from several nm up to 60 nm. Acetonitrile (CH_3CN) is an aprotic organic solvent, which dissolves a wide range of ionic and non-polar compounds. There are different theories how aprotic molecules interact with layered chalcogenide compounds such as MoS_2 and WS_2. It is believed that acetonitrile physisorbs on the sulfur-terminated terraces on MoS_2 or that the MoS_2 lattice may act as a host.[41] Nonetheless, both the mechanisms result in the weakening of van der Waals forces between the layers of MoS_2. Based on this mechanism, acetonitrile-based method offers critical advantage over existing methods by providing large-sized thin layers (high surface to weight ratio). Our protocol when tested using other common solvents yielded similar results (see the supplementary material).[42]

Figures 2(a) and 2(c) present AFM images giving indications about the morphology of flakes obtained. MoS_2 layers typically measure from a few up to 60 μm in length and thicknesses in the range of 15–45 nm, as can be extracted from the height profile in Fgure 2(b). A closer look at the

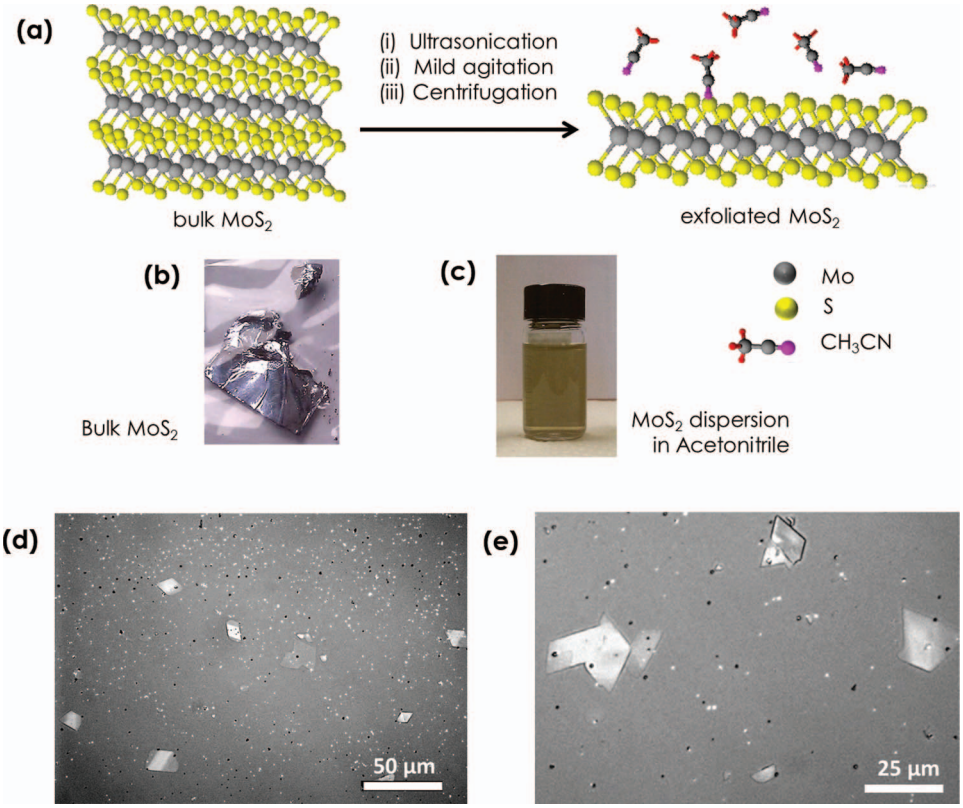

FIG. 1. Chemical exfoliation of bulk MoS_2 in Acetonitrile. (a) Schematic showing the exfoliation process. (b, c) Photos showing the starting MoS_2 crystal and the final dispersion, respectively. (d, e) Optical images of MoS_2 flakes obtained after drop-casting the dispersion.

edge of the flakes (Figure 2(c)) reveals rather fine details, where steps and terraces are visible. From the height profile (Figure 2(d)) in this region, a step size of 3 nm can be extracted. This corresponds to 4 monolayers of MoS_2 (approx. 0.8 nm $\times$ 4 nm). Figure 2(e) shows absorption spectra of MoS_2 suspension in acetonitrile, where four absorption bands can be discerned. The bands A1 (1.834 eV, 676 nm) and B1 (2.01 eV, 617 nm) are attributed to excitonic absorption arising due to the direct bandgap at the K-point.[43] The double bands and characteristic spacing of 0.18 eV between them arise due to interlayer *d-d* interactions and spin orbit splitting.[44,45] As suggested by the recent calculations for the absorption spectra of bilayer and multilayer MoS_2, excitonic peaks D (3 eV, 406 nm), and C (2.7 eV, 460 nm) can be attributed to the existence of high density of states arising due to parallel conduction and valance bands between K and Γ points of the Brillouin zone.[46]

With the aim of realizing thin layer MoS_2 devices, microelectrodes patterned glass chips were used. The MoS_2 flakes were trapped from their dispersion onto the microelectrode gaps (typically 3 μm) using AC dielectrophoresis. For this purpose, a small droplet of the MoS_2 dispersion was placed on the electrode gap while applying 5 V AC signal at a frequency of 5 MHz for 30 s using a function generator. A non-uniform electrical field generated between the electrodes leads to positive dielectrophoretic force acting on the flakes in dispersion.[30] As a result flakes are pulled towards the electrode gap and immobilize forming a bridge between the pair of electrodes. A schematic of the chip layout and the trapping configuration is shown in Figure 3(a). Figure 3(b) presents AFM image of a typical MoS_2 device fabricated in this manner where a MoS_2 flake is deposited over the gap between the source and drain electrodes and covering them partially. Figure 3(c) illustrates height profile of the deposited flake across a line as shown in the AFM image, with a thickness measured around 10 nm. As-fabricated devices were highly resistive (typically ranging from hundreds of megaohms up to a couple of giga ohms) most likely due to poor contacts at the electrodes. To

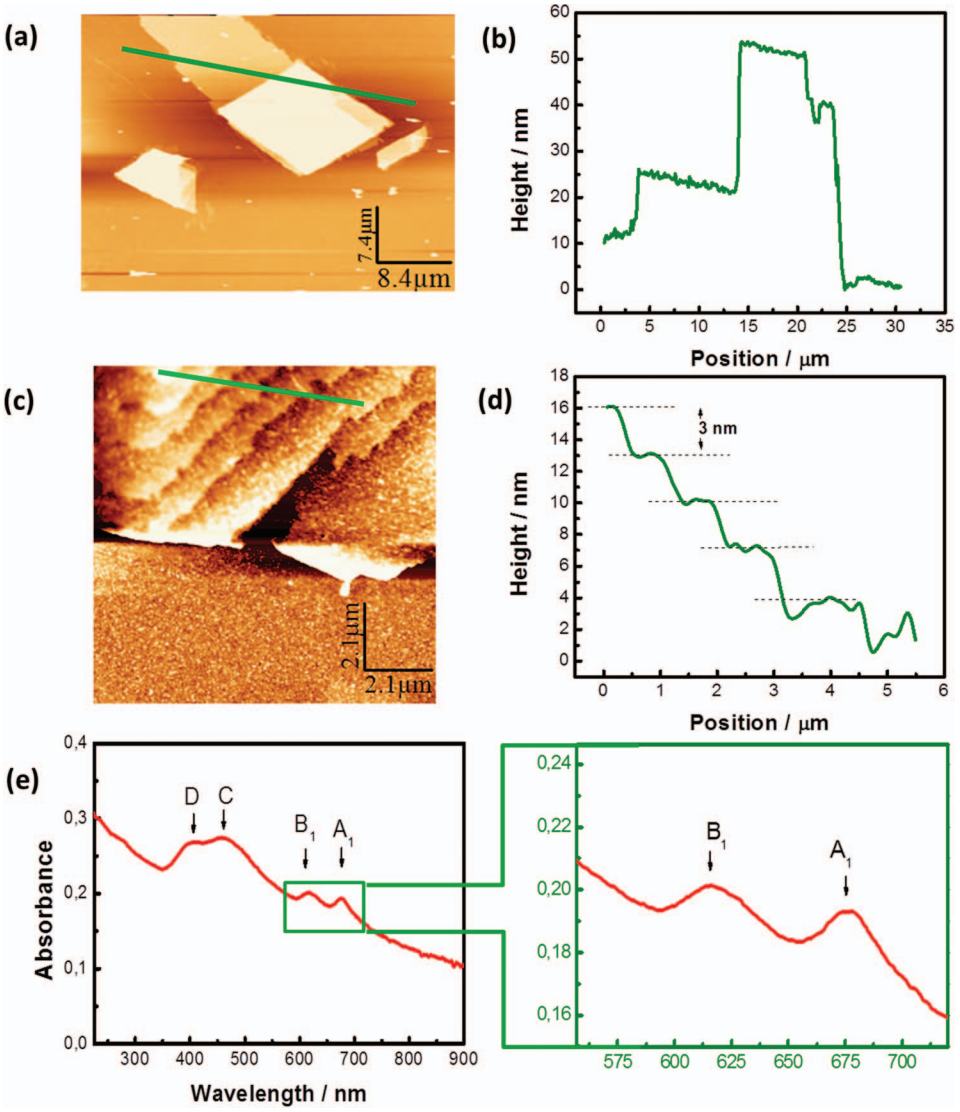

FIG. 2. Characterization of the thin-layer MoS_2 flakes. (a, c) Atomic force microscope images of MoS_2 flakes drop-casted on glass samples. (b, d) Height profiles across the lines shown in the images (a) and (c), respectively. The thickness of flakes in (a) was measured to be around 15 nm. (c, d) Steps and terraces are visible at the edge region with a step size of 3 nm corresponding to 4 monolayers of MoS_2. (e) UV-VIS-Absorption spectrum of MoS_2 in acetonitrile. The inset shows a zoom-in of the excitonic bands typically observed in MoS_2 layers.

improve the contact resistances, the devices were annealed at 300 °C for 3 h in H_2/Ar environment, after which they showed low resistances and were subsequently used for the rest of the measurements. Smaller MoS_2 flakes exfoliated in other solvents such as NaOH, Dimethylsulphoxide (DMSO), and soldiumdodecylsulfonate (SDS) were also deposited on to chips in a similar way.[42]

Figure 4 collects the results obtained from field-effect measurements of such devices in liquid. Schematics and a photo of the liquid-gating measurement setup is shown in Figures 4(a) and 4(b), respectively, where it can be seen that the glass samples are equipped on top with a microwell cast out of a polydimethylsiloxane (PDMS) layer. The microwell aligned exactly around the transport channel of the device minimizes the contact of liquid to the electrode lines, provides for better handling of liquid and for facile positioning of a gate electrode. A Ag/AgCl reference electrode is placed in the micro-well working as the gate electrode. Figure 4(c) shows the field-effect characteristics of one of the devices with a typical *n*-type behavior and an ON-OFF current ratio of around 2

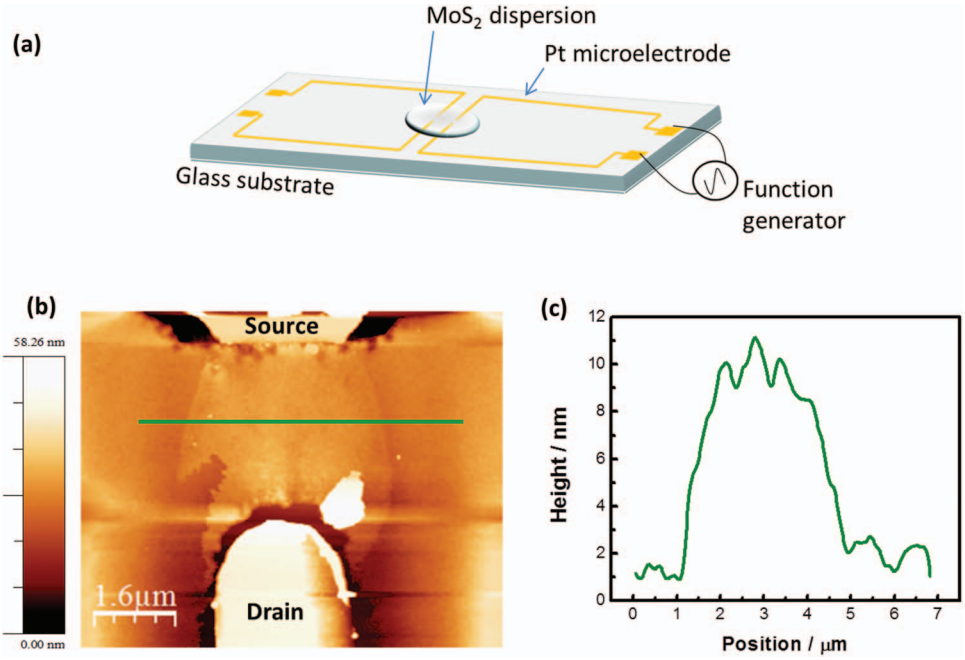

FIG. 3. Dielectrophoretic fabrication of electrical devices using chemically exfoliated MoS_2. (a) Schematic of the layout and the setup for AC dielectrophoresis. (b) AFM image of a typical MoS_2 device showing selective deposition of a flake bridging the microelectrode gap. (c) Height profile along the line in (b) indicating a flake thickness of around 10 nm.

orders of magnitude. Sub-threshold swing as low as 176 mV/decade was extracted for this device. The field-effect mobility (μ) of this device was calculated to be around 0.423 $cm^2\,V^{-1}\,S^{-1}$ using $\mu = dI/dV.L/(c_{edl}.V_{ds})$, where dI/dV is transconductance (S) of the devices, L is channel length ($\sim 3\ \mu m$), V_{ds} is drain-source bias, and c_{edl} is electrical double layer capacitance (EDLC). EDLC was calculated using the equation for sheet capacitance ($c = \varepsilon_0.\varepsilon_r.A/d$ where ε_0 is permittivity of free space, ε_r is relative permittivity of buffer solution, A is the area of channel and d is the thickness of EDL). Typical field-effect mobilities calculated here were comparably larger than that of similar devices reported recently. Higher field-effect mobilities could be attributed to device operation in liquid medium where an electrical double layer capacitance is the key for producing field-effect. Longer channel lengths of our devices, smaller flake thicknesses, mild exfoliation method, and cleaner device fabrication processes reducing the amount of impurities on MoS_2 flakes may be helpful in increasing the field-effect mobility values.[47] Among other aspects except for constructing fast electronic circuits for various applications, devices with high mobilities are also expected to exhibit higher sensitivities for sensing purposes.[48–51]

The devices were subsequently evaluated as chemical sensors in liquids. In order to demonstrate the sensing characteristics of the devices, we exposed them to phosphate buffer solutions of varying pH. The field-effect behavior in different pH solutions is shown in Figure 4(d) for pH values ranging from 7.0 to 9.8. The threshold values for each conductance curve at different pH values were ascertained by extrapolation of the linear regime of the gate dependence characteristics.[42,52] It is apparent that the threshold voltages shift to more positive gate voltages as the pH is increased. This shift can be attributed to variations in the surface charge present on the MoS_2 flakes. It can be expected that when MoS_2 is annealed in H_2/Ar atmosphere, the surface is filled with –SH (thiol) moieties.[23] The thiol groups have an isoelectric point of around 10, which results in an increase in negative surface charge as the pH is increased. The threshold voltage shift in Figure 4(d) is extracted to obtain the calibration curve in Figure 4(e) showing the pH response with a sensitivity of around 53 mV/pH.

The direct bandgap in MoS_2 motivates the investigation of the effect of photo illumination on the electrical characteristics of the fabricated devices. Towards this aim, we have measured the

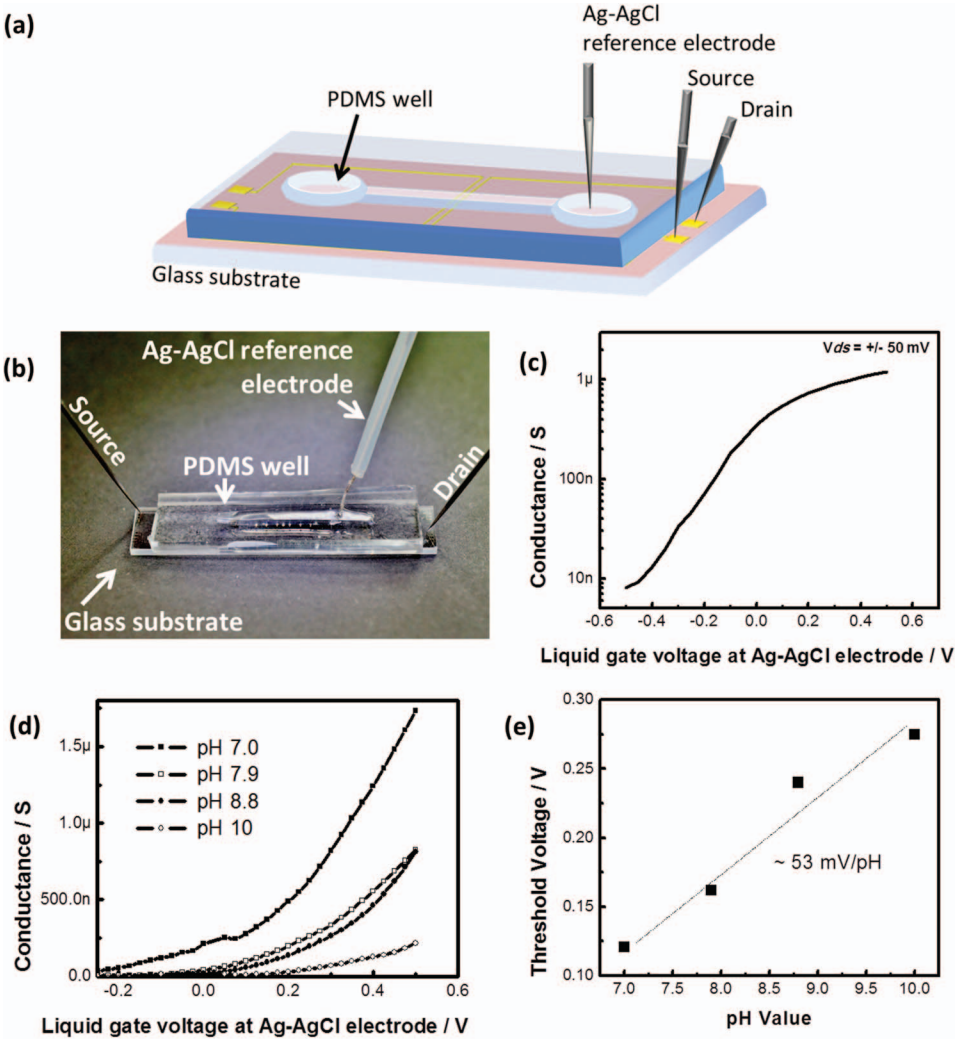

FIG. 4. Field effect behavior of MoS_2 flakes in liquids. (a) The schematics of the measurement setup. (b) Photo of the liquid gating setup where a PDMS well is mounted on the chip, along with the source and drain leads and the Ag/AgCl reference electrode (gate). (c) Field-effect characteristics of a typical device in water showing *n*-type behavior with ON-OFF ratio of around 2 orders of magnitude. (d) Field-effect characteristics of the same device when immersed in buffer solutions of different pH values. (e) Calibration curve showing the pH sensor response where the threshold voltage is plotted as a function of pH.

resistance of the devices in the dark and under illumination from a laser diode in air. We used an excitation wavelength of 658 nm (elliptical spot –2 mm × 1 mm, max. intensity 1.54 W/cm^2) in order to mainly excite the A1 transition. Figure 5(a) presents typical current-voltage (I-V) characteristics with and without laser irradiation showing a clear decrease in resistance by around 2 orders of magnitude upon photo illumination. This behavior is further confirmed from the temporal responses in Figure 5(b), where short laser pulses were used while measuring the conductivity of the sample. We attribute the decrease in resistance to photoconductivity in the trapped MoS_2 flakes. At the A1 transition, the laser generates excitons, which are subsequently separated by the electric field due to the drain source bias. It is apparent that the switching of the resistance is rather quick (within the time resolution of our measurement –100 ms), although a slight relaxation can be seen when the laser is switched off. This suggests that other mechanisms (such as photodesorption or photoactivated chemical reactions) if present have only small effects. Further support for this can also be obtained from the magnitude of laser-induced conductance, which is rather constant over all the cycles shown

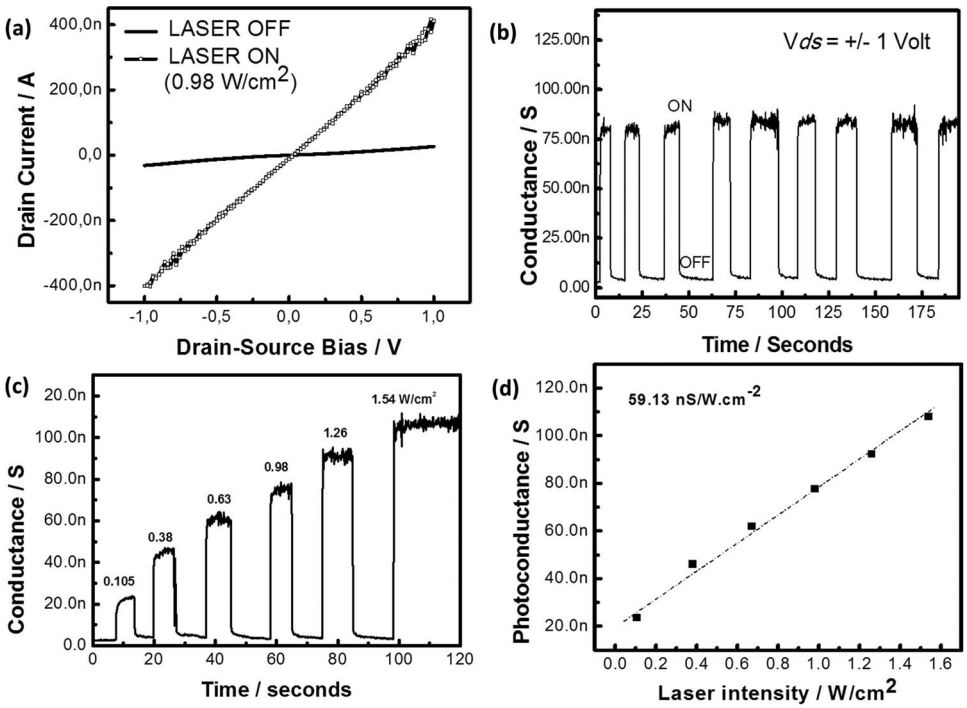

FIG. 5. Photoconductivity in thin layer MoS_2 devices. (a) Current-voltage curves in the dark (solid black curve) and under photo illumination (curve with hollow circles) showing an increase in conductance upon photo illumination. (b) Conductance of a typical device during several switching cycles (laser ON and OFF), the drain-bias here is ± 1 V. (c) Conductance of the device with repeated ON/OFF cycles of increasing laser intensity. The drain-source bias is $\pm$ 1 V. (d) The photoconductance from (c) is plotted here as a function of laser intensity showing a linear response.

here. Moreover, a linear increase in the photoconductance response is observed as the intensity of the laser is increased as shown in Figures 5(c) and 5(d). The linear increase in the photoconductance with optical power suggests that the generation of photocurrent is mostly occurring by the irradiated photons.[53] However, the exact location of exciton generation (namely, at the middle of the flake or at the Schottky barrier at the contacts) cannot be discerned from these experiments. Spatially resolved photocurrent measurements may shed light on this aspect in the future.[54,55]

In conclusion, we have presented a versatile approach for the fabrication of 2D MoS_2 devices with interesting electrical and optoelectronic properties. We have optimized a solution-based exfoliation method for MoS_2 yielding thin flakes of large sizes. The proposed protocol may find use in fabricating devices in a scalable manner in order to study the physical properties more systematically and to optimize them for a specific application. As a proof of concept towards practical applications, we have shown two examples, namely, a chemical sensor operating in liquids to detect pH and a photo resistor with a strong and quick photo response. The simplicity of the protocol and the ability to obtain devices with large flakes will have an important impact for future applications in electronics, chemical sensing, and optoelectronics.

MoS_2 crystals were purchased from SPI supplies Canada. Crystals were first cut into smaller pieces using a scalpel and taken into glass vial filled with 40 ml acetonitrile. The mixture was mildly ultrasonicated for 30 min at 50 °C which turns turbid due to dissolution of MoS_2. Mixture was shaken on mini-rotor for 9 h at 200 rpm followed by mild ultrasonication for 30 min and a shaking step of 1 h when the solution was put to rest till residual MoS_2 separated from the solution and settled down. MoS_2 thin-layers were obtained from this dispersion. The MoS_2 dispersion was centrifuged at 4600 rpm for 5 min to remove big crystallites. Methods of structural characterization of MoS2 flakes, dielectrophoretic deposition and transport characterization of devices are discussed in detail in the supplementary material.[42]

This project was funded from the German ministry for Education and Research (BMBF) under the NanoFutur programme (O3×5516).

[1] K. S. Novoselov, D. Jiang, F. Schedin, T. J. Booth, V. V. Khotkevich, S. V. Morozov, and A. K. Geim, Proc. Natl. Acad. Sci. U.S.A. **102**, 10451 (2005).
[2] R. Mas-Ballesté, C. Gómez-Navarro, J. Gómez-Herrero, and F. Zamora, Nanoscale **3**, 20 (2011).
[3] Y. Zhang, Y.-W. Tan, H. L. Stormer, and P. Kim, Nature (London) **438**, 201 (2005).
[4] A. Geim and K. Novoselov, Nature Mater. **6**, 183 (2007).
[5] A. H. Castro Neto, N. M. R. Peres, K. S. Novoselov, and A. K. Geim, Rev. Mod. Phys. **81**, 109 (2009).
[6] P. K. Ang, W. Chen, A. T. S. Wee, and K. P. Loh, J. Am. Chem. Soc. **130**, 14392 (2008).
[7] Y.-W. Son, M. Cohen, and S. Louie, Phys. Rev. Lett. **98**, 089901 (2007).
[8] M. Y. Han, B. Ozyilmaz, Y. Zhang, and P. Kim, Phys. Rev. Lett. **98**, 206805 (2007).
[9] Y. Zhang, T.-T. Tang, C. Girit, Z. Hao, M. C. Martin, A. Zettl, M. F. Crommie, Y. R. Shen, and F. Wang, Nature (London) **459**, 820 (2009).
[10] G. Giovannetti, P. Khomyakov, G. Brocks, P. Kelly, and J. van den Brink, Phys. Rev. B **76**, 073103 (2007).
[11] J. K. Ellis, M. J. Lucero, and G. E. Scuseria, Appl. Phys. Lett. **99**, 261908 (2011).
[12] S. Han, H. Kwon, S. Kim, S. Ryu, W. Yun, D. Kim, J. Hwang, J. S. Kang, J. Baik, H. Shin, and S. Hong, Phys. Rev. B **84**, 045409 (2011).
[13] B. Radisavljevic, M. B. Whitwick, and A. Kis, ACS Nano **5**, 9934 (2011).
[14] F. Schwierz, Nat. Nanotechnol. **6**, 135 (2011).
[15] Y. Zhang, J. Ye, Y. Matsuhashi, and Y. Iwasa, Nano Lett. **12**, 1136 (2012).
[16] H. Li, Z. Yin, Q. He, H. Li, X. Huang, G. Lu, D. W. H. Fam, A. I. Y. Tok, Q. Zhang, and H. Zhang, Small Weinheim an Der Bergstrasse Germany **8**, 63 (2012).
[17] A. Splendiani, L. Sun, Y. Zhang, T. Li, J. Kim, C.-Y. Chim, G. Galli, and F. Wang, Nano Lett. **10**, 1271 (2010).
[18] Z. Yin, H. Li, H. Li, L. Jiang, Y. Shi, Y. Sun, G. Lu, Q. Zhang, X. Chen, and H. Zhang, ACS Nano **6**, 74 (2012).
[19] G. Eda, H. Yamaguchi, D. Voiry, T. Fujita, M. Chen, and M. Chhowalla, Nano Lett. **11**, 5111 (2011).
[20] M. B. P. Fontana, T. Deppe, A. K. Boyd, M. Rinzan, A. Y. Liu, and M. Paranjape, Sci. Rep. **3**, 1634 (2013).
[21] L. Liu, S. B. Kumar, Y. Ouyang, and J. Guo, IEEE Trans. Electron Devices **58**, 3042 (2011).
[22] Y. Yoon, K. Ganapathi, and S. Salahuddin, Nano Lett. **11**, 3768 (2011).
[23] L. S. Byskov, M. Bollinger, J. K. Nørskov, B. S. Clausen, and H. Topsøe, J. Mol. Catal. A: Chem. **163**, 117 (2000).
[24] A. O. Neill, U. Khan, and J. N. Coleman, Chem. Mater. **24**, 2414 (2012).
[25] Z. Wang, T. Chen, W. Chen, K. Chang, L. Ma, G. Huang, D. Chen, and J. Y. Lee, J. Mater. Chem. A **1**, 2202 (2013).
[26] K.-K. Liu, W. Zhang, Y.-H. Lee, Y.-C. Lin, M.-T. Chang, C.-Y. Su, C.-S. Chang, H. Li, Y. Shi, H. Zhang, C.-S. Lai, and L.-J. Li, Nano Lett. **12**, 1538 (2012).
[27] A. Castellanos-Gomez, M. Barkelid, A. M. Goossens, V. E. Calado, H. S. J. Van Der Zant, and G. A. Steele, Nano Lett. **12**, 3187 (2012).
[28] Y. Shi, W. Zhou, A. Lu, W. Fang, Y. Lee, A. L. Hsu, S. M. Kim, K. K. Kim, H. Y. Yang, L. Li, J. Idrobo, and J. Kong, Nano Lett. **12**, 2784 (2012).
[29] T. Kurkina, S. Sundaram, R. S. Sundaram, F. Re, M. Masserini, K. Kern, and K. Balasubramanian, ACS Nano **6**, 5514 (2012).
[30] B. R. Burg and D. Poulikakos, J. Mater. Res. **26**, 1561 (2011).
[31] F. R. Gamble, J. H. Osiecki, M. Cais, R. Pisharody, F. J. Disalvo, and T. H. Geballe, Science **174**, 493 (1971).
[32] W. M. Divigalpitiya, R. F. Frindt, and S. R. Morrison, Science **246**, 369 (1989).
[33] J. P. Lemmon and M. M. Lerner, Chem. Mater. **6**, 207 (1994).
[34] M. N. Tahir, N. Zink, M. Eberhardt, H. A. Therese, U. Kolb, P. Theato, and W. Tremel, Angew. Chem., Int. Ed. **45**, 4809 (2006).
[35] G. G. Ruiz-Hitzky Eduardo, J. Ricardo, C. Blanca, M. Victor, and S. A. Angelica, Adv. Mater. **5**, 738 (1993).
[36] E. Benavente, M. A. S. Ana, F. Mendiza, and G. Gonza, Coord. Chem. Rev. **224**, 87 (2002).
[37] R. J. Smith, P. J. King, M. Lotya, C. Wirtz, U. Khan, S. De, A. O'Neill, G. S. Duesberg, J. C. Grunlan, G. Moriarty, J. Chen, J. Wang, A. I. Minett, V. Nicolosi, and J. N. Coleman, Adv. Mater. **23**, 3944 (2011).
[38] V. Sanchez, E. Benavente, M. A. S. Ana, and G. Gonzalez, Chem. Mater. **11**, 2296 (1999).
[39] G. Gonzáleza, A. M. A. Santa, and E. Benavente, Electrochim. Acta **43**, 1327 (1998).
[40] J. N. Coleman, M. Lotya, A. O'Neill, S. D. Bergin, P. J. King, U. Khan, K. Young, A. Gaucher, S. De, R. J. Smith, I. V. Shvets, S. K. Arora, G. Stanton, H.-Y. Kim, K. Lee, G. T. Kim, G. S. Duesberg, T. Hallam, J. J. Boland, J. J. Wang, J. F. Donegan, J. C. Grunlan, G. Moriarty, A. Shmeliov, R. J. Nicholls, J. M. Perkins, E. M. Grieveson, K. Theuwissen, D. W. McComb, P. D. Nellist, and V. Nicolosi, Science **331**, 568 (2011).
[41] K. E. Dungey, M. D. Curtis, and J. E. Penner-hahn, Chem. Mater. **10**, 2152 (1998).
[42] See supplementary material at http://dx.doi.org/10.1063/1.4820423 for the chemical exfoliation of MoS_2 flakes in other solvents, methods for structural characterization, details of dielectrophoretic deposition over different substrates and methods for device charcaterization.
[43] A. K. M. Newaz, D. Prasai, J. I. Ziegler, D. Caudel, S. Robinson, R. F. Haglund, Jr., and K. I. Bolotin, Solid State Commun. **155**, 49 (2013).
[44] R. Coehoorn, C. Haas, J. Dijkstra, and C. J. F. Flipse, Phys. Rev. B **35**, 6195 (1987).
[45] Y. Fong and M. Schlüter, *Electrons and Phonons in Layered Crystal Structures* (Reidel, Dordrecht, 1979), p. 145.
[46] A. Molina-Sanchez, D. Sangalli, K. Hummer, A. Marini, and L. Wirtz, Phys. Rev. B **88**, 045412 (2013).
[47] K. Lee, H.-Y. Kim, M. Lotya, J. N. Coleman, G.-T. Kim, and G. S. Duesberg, Adv. Mater. **23**, 4178 (2011).
[48] S. Wang, P. K. Ang, Z. Wang, A. L. L. Tang, J. T. L. Thong, and K. P. Loh, Nano Lett. **10**, 92 (2010).

[49] M. J. Allen, V. C. Tung, and R. B. Kaner, Chem. Rev. **110**, 132 (2010).
[50] R. S. Friedman, M. C. McAlpine, D. S. Ricketts, D. Ham, and C. M. Lieber, Nature (London) **434**, 1085 (2005).
[51] V. Pachauri, K. Kern, and K. Balasubramanian, Appl. Phys. Lett. **102**, 023501 (2013).
[52] A. Ortiz-Konde, F. J. Garcia Sanchez, J. J. Liou, A. Cerdeira, M. Estrada, and Y. Yue, Microelectron. Reliab. **42**, 583 (2002).
[53] S. M. Sze and K. K. Nag, *Physics of Semiconductor Devices*, 3rd ed. (Wiley, New York, 2007).
[54] E. J. H. Lee, K. Balasubramanian, R. T. Weitz, M. Burghard, and K. Kern, Nat. Nanotechnol. **3**, 486 (2008).
[55] J. Park, Y. H. Ahn, and C. Ruiz-Vargas, Nano Lett. **9**, 1742 (2009).